Journal of Power Sources 268 (2014) 895–903

Contents lists available at ScienceDirect

Journal of Power Sources

journal homepage: www.elsevier.com/locate/jpowsour

Remaining capacity estimation of Li-ion batteries based on temperature sample entropy and particle filter

Junfu Li, Chao Lyu*, Lixin Wang, Liqiang Zhang, Chenhui Li

School of Electrical Engineering and Automation, Harbin Institute of Technology, Harbin 150001, China

HIGHLIGHTS

- Relationship between surface temperature and discharge capacity is found via SampEn.
- Functional relationship between multi-variables and discharge capacity is obtained.
- A model of remaining capacity estimation based on SampEn and PF is proposed.
- Estimation performs quite well on various operating conditions.

ARTICLE INFO

Article history:
Received 15 April 2014
Received in revised form
29 May 2014
Accepted 24 June 2014
Available online 7 July 2014

Keywords:
Thermal stability
Remaining capacity
Sample entropy
Particle filter

ABSTRACT

Currently, safety issue on Li-ion battery caused by thermal stability is one of the main factors that restricts its developmental application. In this paper, from a perspective of heat generation, we present a method to estimate remaining capacity of single Li-ion battery. Sample entropy (SampEn) is employed for the calculation of surface temperature in charging process and the relationship between SampEn and capacity fading in aging process is built. Considering various factors of capacity attenuation, an intelligent estimation approach is proposed by the combination of SampEn and particle filter (PF).

1. Introduction

Safety issue related to Li-ion battery is mainly caused by (i) acupuncture, extruding, or thermal shock that may result in internal short circuit and produce quantity of heat, (ii) irreversible thermal chemical reaction in overcharging process, (iii) and thermal runaway caused by Li-ion deintercalation of positive material [1]. In the case of abuse, li-ion battery may even reach the temperature (>700 °C) that is high enough to melt the aluminum collector. As a result, cells would likely be on fire or even explode [2].

Generally, thermal stability of battery materials is an important property in terms of safety. As Li-ion transmits between anode and cathode electrodes, numerous physical and chemical reactions raise the internal temperature of battery. Meanwhile, due to the elevated temperature, many additional exothermic reactions occur and further raise the internal temperature. The main exothermic reactions caused by increasing temperature include decomposition of SEI film, electrolyte, and positive electrode, as well as the reaction of negative electrode and electrolyte or binder [1]. In addition, as battery materials (electrolyte, separator, SEI film, etc.) block the transmitting of Li^+, a small amount of heat will be generated. Li-ion battery attenuation of capacity is closely related to temperature. At high temperature, capacity decreases faster than in normal condition on account of a high-rate dissolution of battery materials and an additional consumption of Li^+. Low temperature results in a slower Li-ion diffusion into carbon as well as diffusion in the electrolyte. Consequently, metallic lithium plating and lithium dendrite growth also lead to consumption of Li^+ and capacity fading [3,4].

Many literatures introduce approaches to estimate capacity of battery. The frequently used method based on principle to analyze the law of battery aging is incremental capacity analysis (ICA). In Ref. [5], ICA along with other electrochemical techniques were used to analyze the degradation process of two types of 10 Ah single cells

* Corresponding author. Harbin Institute of Technology, No. 92, West Dazhi Street, P.O. Box 404, Nangang District, Harbin 150001, Heilongjiang, PR China. Tel.: +86 18646386016; fax: +86 0451 86402965.
E-mail addresses: 13B906023@hit.edu.cn (J. Li), lu_chao@hit.edu.cn (C. Lyu), wlx@hit.edu.cn (L. Wang), zhang.lq@hit.edu.cn (L. Zhang), huihui11_27@163.com (C. Li).

http://dx.doi.org/10.1016/j.jpowsour.2014.06.133
0378-7753/

tested at room temperature and 60 °C. The analysis illustrated a unique capability of using ICA to differentiate cell performance and material utilization in different cell designs. In Ref. [6], two stages of degradation were observed in the life cycle under certain aging regime and a detailed explanation for capacity fade in each stage was also made. Although mechanism-based method is precise and acceptable when describing aging process from the aspect of internal degradation mechanism, it involves numerous simulating calculations.

Model-based estimation refers to the method of dynamic process, such as physical model method, Kalman or extended Kalman filter (EKF), PF, and the theory based on expertise [7]. An integrated methodology of prognosis for electrical components based on physical failure models and Bayesian estimation methods was introduced in Ref. [8]. Furthermore, an empirical formula was proposed to describe the law of Li-ion battery capacity fading and simulation results indicated that PF algorithm was appropriate for state of health (SOH) estimation in Refs. [9–11]. In Ref. [12], several algorithms were presented, including method of autoregressive integrated moving average (ARIMA), relevance vector machine (RVM), EKF, and PF. The RVM–PF framework had significant advantages over conventional remaining useful life (RUL) estimation methods such as ARIMA and EKF. The advantage of PF is that it is no longer limited to the fact that random variables must satisfy the condition of Gaussian distribution. This technology is applicable to non-Gaussian and nonlinear random system which can be described as a state space model. Model-based method can effectively avoid study on complicated mechanism and it is easy to achieve. However, it requires certain amount of data and the estimation results usually come with larger errors.

Feature-based method has great actual significance. Compared to complicated electrochemical mechanism of battery, aging features are more comprehensible and relatively easier to be captured. Impedance characteristics are deemed to be features of battery life in many previous literatures. Salkind et al. [13] proposed a practical method that resistances were obtained by electrochemical impedance spectroscopy (EIS) measurement and coulomb counting techniques were employed to predict state of charge (SOC). The advantage of this work was that there was no need to know previous discharge or cycling history. Gomez et al. [14] made a detailed analysis on EIS and pointed out that aging information could be embodied by parameters of EIS. In addition, an equivalent circuit model (ECM) was also introduced to describe internal electrochemical properties. More explicitly, parameters in this model were considered to change with aging gradually and were seen as characteristics of battery aging. By monitoring changes of these characteristics, the law of aging process could be captured. Liaw et al. [15] researched on storage life of Li-ion battery at an ambient temperature of 55 °C via ECM. Cell aging process could mainly be reflected by minor changes of some parameters. The results showed that such an integrated approach could actually lead to a high-fidelity simulation of battery performance and life.

Some researchers also extracted aging information from current and voltage curves during charging or discharging process. Sun et al. [16] presented an intelligent aging estimation method based on SampEn which could serve as an indicator for the degradation of the lead-acid battery. Aging information was extracted from discharging voltage and the proposed method provided expected results and applicability. The idea of fusion of feature-based and model-based method was proposed in Refs. [17,18]. As inputs for frameworks of support vector machine (SVM), RVM, or PF, the features of discharging voltage curves were captured through SampEn. The integrated estimation algorithms provided plausible results.

Three kinds of capacity estimation or aging analysis methods of batteries have been mentioned above. The comparison of their strengths and weaknesses is cast for a better overview in Table 1.

Most literatures neglected thermal factors in models mentioned above. Monitoring the surface temperature of battery does not only take the function of safety precaution, but also provides external characteristic information which can be utilized to assess battery SOH. Thus, this work is conducted from the following perspectives. Firstly, it is essential to seek the relationship between discharge capacity and external feature. Secondly, SampEn of charging temperature is calculated and its relationship with capacity is established. Finally, considering various factors related to capacity attenuation, we propose a model of remaining capacity estimation based on the combination of temperature SampEn and PF.

2. Theory and intelligent estimation method

2.1. SampEn

SampEn was developed by Richman and Moorman [19] for signal analysis. It can be expressed as SampEn (m, r, N), where N is a given total number of data, r is the tolerance for accepting matrices, and m is the dimension of vectors. The specific algorithm of SampEn is described as follows. For a given series $\{x_i\}$, we form $N - m + 1$ vectors as:

$$X(i) = [x(i), x(i+1), \ldots, x(i+m-1)], \quad \text{for } i = 1 \text{ to } N - m + 1. \tag{1}$$

The distance between vector $X(i)$ and $X(j)$ is defined as:

$$\mathrm{d}[X(i), X(j)] = \max|x(i+k) - x(j+k)|, \quad \text{for } i, j = 1 \text{ to } N - m + 1, \; k = 0 \text{ to } m - 1. \tag{2}$$

For a given r, calculate the number of $d[X(i), X(j)] < r$, for $i \neq j$, and define the function:

$$B_i^m(r) = \frac{1}{N-m}\mathrm{num}\{\mathrm{d}[X(i), X(j)] < r\}. \tag{3}$$

Then take the average of $B_i^m(r)$. The result is expressed as:

$$B^m(r) = \frac{1}{N-m+1}\sum_{i=1}^{N-m+1} B_i^m(r). \tag{4}$$

Similarly, replace m with $m + 1$ and determine the two values $B^m(r)$ and $B^{m+1}(r)$. Given the data length is always limited, the SampEn is estimated by:

Table 1
Comparison of strengths and weaknesses of each estimation method.

	Mechanism-based method	Model-based method	Feature-based method
Strengths	Precise description of degradation mechanism, clear physical concept	Easily comprehensible with uncomplex mechanism, algorithm easy to achieve	Easily comprehensible with uncomplex mechanism, algorithm easy to achieve
Weaknesses	Complicated mechanism, algorithm difficult to achieve, large amount of simulating calculation	Large amount of data, larger errors	Large amount of data, lack of physical significance of some feature parameters, larger errors

$$\mathrm{SampEn}(m,r,N) = -\ln\left[B^{m+1}(r)\Big/B^{m}(r)\right]. \quad (5)$$

The value of SampEn (m, r, N) is closely correlated with m, r, and N. Fig. 1 shows the flow chart for algorithm and functionality of SampEn.

2.2. PF algorithm

PF is a Bayesian learning technique using Monte Carlo simulations. The idea is to describe the parameters of system state as a probability density function (PDF) approximated by particles that are generated from a priori distribution and updated by a measurement model. Model parameters are included as a part of state vector to be tracked. PF framework can be applied to RUL prediction of battery given its good state tracking performance.

Sequential importance resampling (SIR), a basic algorithm of PF [20], is employed in this paper and the procedure of SIR is cast as below:

(a) *Initialization*: a swarm of points named particles $\{x_0^i\}_{i=1}^N$ are generated and initial importance weight is set to N^{-1}.
(b) *Updating*: at cycle time k, particles are updated by $X_k^i = \pi(X_k^i | X_{0:k-1}^i, y_{1:k})$ and then the weight of each particle is computed.
(c) *Normalization*: normalize the very weights of all particles using the following formula:

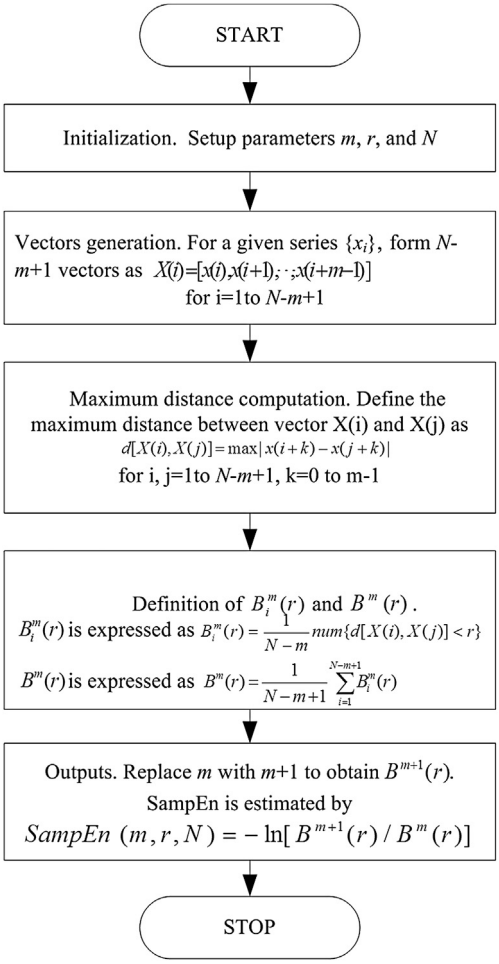

Fig. 1. Flow chart for algorithm and functionality of SampEn.

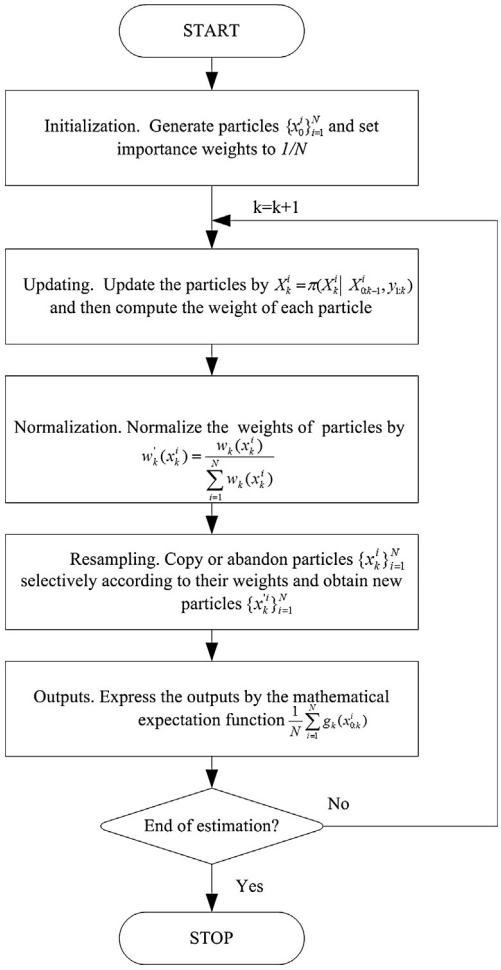

Fig. 2. Flow chart for algorithm and functionality of SIR.

$$w_k'\left(x_k^i\right) = \frac{w_k\left(x_k^i\right)}{\sum_{i=1}^{N} w_k\left(x_k^i\right)}. \quad (6)$$

(d) *Resampling*: through sampling method, each particle $\{x_k^i\}_{i=1}^N$ is copied or abandoned selectively according to its weight. Then new particles $\{x_k^i\}_{i=1}^N$ are obtained.
(e) *Outputs*: the outputs of PF algorithm can be approximately expressed by the mathematical expectation function $1/N\sum_{i=1}^N g_k(x_{0:k}^i)$, where $g_k(x_{0:k})$ represents a specific function of particles.
(f) Let $k = k + 1$ and go back to step (b).

Fig. 2 shows the flow chart for algorithm and functionality of SIR.

Table 2
The selected numbers and operating conditions of testing batteries.

Battery number	Ambient temperature (°C)	Discharge current (A)	Cut-off voltage (V)	Terminal condition
27	24	4 A 0.05 Hz square	2.5	30% Fade
31	43	4	2.5	30% Fade
34	24	4	2.2	20% Fade
36	24	2	2.7	20% Fade
51	4	2	2.5	Crashed
55	4	2	2.5	30% Fade

2.3. Model of remaining capacity estimation

2.3.1. Relationship between temperature SampEn and discharge capacity

Since internal failure mechanism of battery is complex and all factors in electrical, thermal, and chemical domains contribute to capacity decay, on-line and real-time monitoring of physical parameters seems to be a big challenge right now. In practical usage, health information of battery is commonly extracted from external features including voltage, current, surface temperature, and impedance. Naturally, the easy way to describe the law of capacity fading is to find the changes of these features at different aging stage. It should be emphasized that temperature SampEn does reflect the aging process along with increasing cycles rather than quantitatively compute the heat produced in physical or chemical exothermic reactions. It removes the need of knowing the mechanism of heat generation, diffusion from interior to surface, and even battery aging mechanism.

Via data fitting, a functional relationship between temperature SampEn and discharge capacity is established. It is apparent

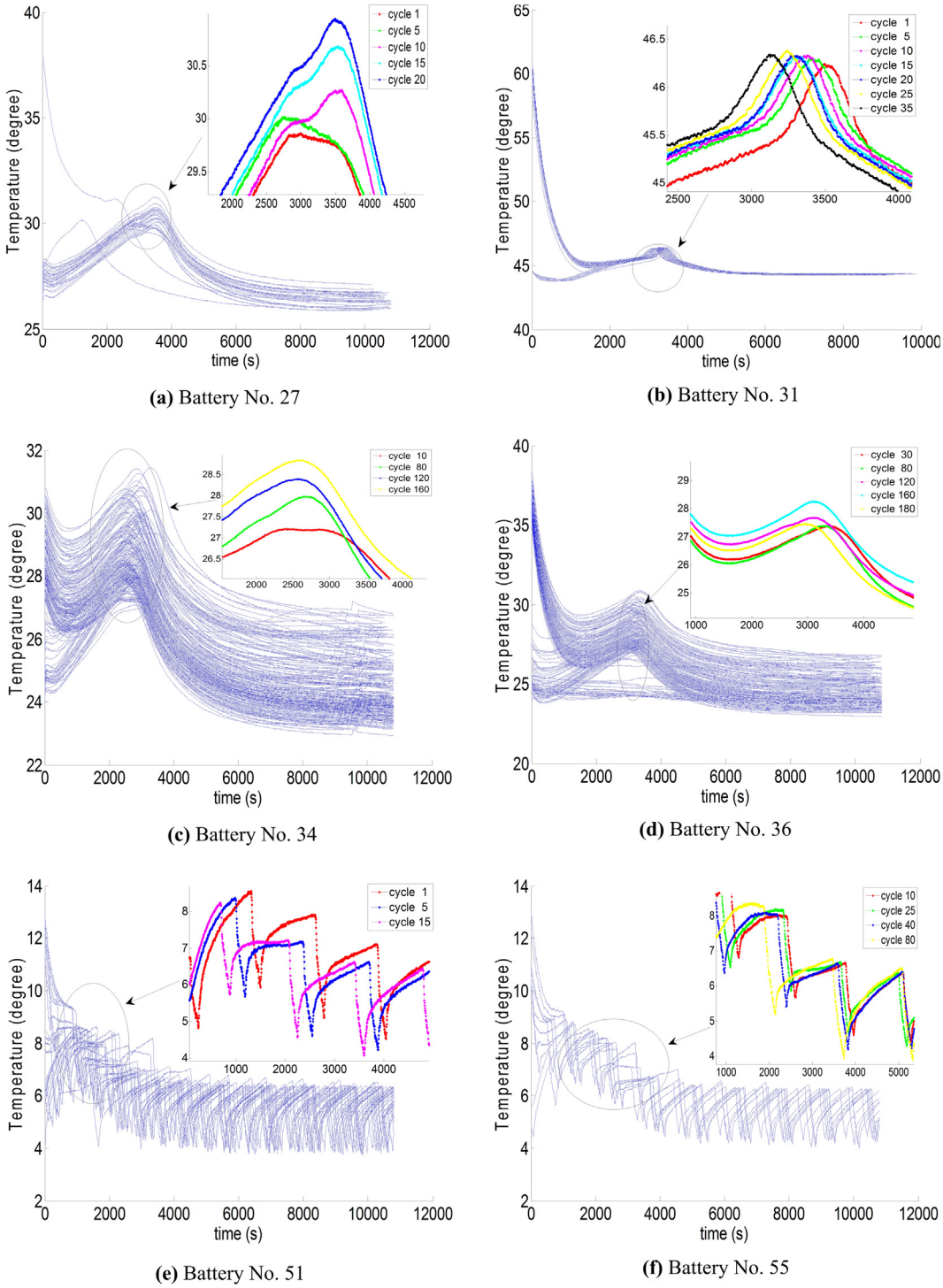

(a) Battery No. 27

(b) Battery No. 31

(c) Battery No. 34

(d) Battery No. 36

(e) Battery No. 51

(f) Battery No. 55

Fig. 3. Changes of surface temperature with time in different cycles.

that charging directly determines the discharge capacity in one cycle. Besides, reaction products forming up around the electrodes will decompose during rest or relaxation period, which leads to an increase of available capacity in the next cycle. Consequently, it is necessary to take these factors into consideration to guarantee fitting accuracy. That is to say, charge capacity and rest time are also considered as fitting independent variables. After each charging cycle, temperature SampEn can be computed and charge capacity is obtained by integrating current curve. The two variables as well as rest time are substituted into the function and the output is regarded as a preliminary capacity estimation result. It is worth mentioning that more historical data contribute to more precise fitting parameters and accurate estimation results.

2.3.2. Intelligent algorithm of estimation

It is known that importance weight of each particle is directly related to observed values in PF of SIR. So the former capacity estimation results serve as observed values. Considering the main influence factors of battery capacity, the following state equations are cast to describe the model as:

$$C'_k = \beta_1(k)C_k + \beta_2(k)\exp(\beta_3(k)/\Delta T_k), \tag{7}$$

$$\beta_i(k+1) = \beta_i(k) + v_i(k), \quad i = 1,2,3 \tag{8}$$

where k is cycle index, C_k denotes the charge capacity, C'_k is the discharge capacity; ΔT_k is the time interval between charge and discharge cycle, β_1, β_2, and β_3 are parameters of the state equation, and v_1, v_2, and v_3 are independent zero-mean Gaussian noise terms.

The procedure of intelligent algorithm of estimation is given as below:

(1) Data collection
   (a) Starting point T is set in proportion to the length of all historical data. The part from the first cycle to T is regarded as known to researchers.
   (b) Extract battery charging temperature curves and relaxation time. Selected parameters m and r are 4 and 0.05, respectively. Compute values of charging temperature SampEn. With several variables mentioned above, a fitting function is obtained.

(2) Parameter initialization
   (a) Obtain initial parameters β_i (i = 1, 2, 3) via fitting;
   (b) 500 initial particles are generated with values obtained in (2)-(a) and the variances of noise term v_i (i = 1, 2, 3) are about 10,000 times smaller than β;

(3) Prediction
   (a) Particles$\{x_k^i\}_{i=1}^N$ are updated by Eq. (8) and the priori discharge capacity values in cycle $k+1$ are calculated through updated particles $\{x_{k+1}^i\}_{i=1}^N$;
   (b) Take SampEn feature, charge capacity and rest time as the inputs of fitting function and compute the weight of each particle per deviation between the observation and previous calculated value. Normalize very particles by Eq. (6);
   (c) Through the method of random sampling, each particle $\{x_{k+1}^i\}_{i=1}^N$ is copied or abandoned selectively according to its weight and then new sample $\{x_{k+1}^{i'}\}_{i=1}^N$ is obtained;
   (d) The average of sample $\{x_{k+1}^{i'}\}_{i=1}^N$ represents the probability density distribution expectation of each parameter in Eq. (7). Then, the final estimation C'_{k+1} can easily be figured up;
   (e) Repeat the steps from (3)-(a) to (3)-(d) until the capacity reaches to its criterion.

3. Data sources

The full set of aging data collected from commercially available 18,650-size lithium-ion cells provided by NASA Ames Prognostics Center of Excellence is taken as object of study. Positive and negative materials are mostly $LiNi_{0.8}Co_{0.15}Al_{0.05}O_2$ and MAG-10 graphite, respectively. The electrolyte is 1.2 M $LiPF_6$ in EC:EMC (3:7 wt %) and the separator is 25 μm thick PE. The nominal capacity and voltage are 2 Ah and 3.7 V, separately. Measured voltages are ranged from 4.2 V to approximate 2.5 V.

All testing batteries were run through different working profiles (charge, discharge, and impedance). Batteries were tested by the following steps: (1) charging was carried out in a constant current mode at 1.5 A until the battery voltage reached 4.2 V, (2) a constant voltage mode was then in operation until the charging current dropped to 20 mA, (3) batteries were put aside for a period of time, (4) impedance measurement was implemented with EIS frequency sweep from 0.1 Hz to 5 kHz, (5) discharging was carried out at a constant current level until the battery voltage fell to the given value. Repeated charging and discharging processes resulted in accelerated aging. The experiments were terminated when the batteries reached the end-of-life criteria, 20–30% fading of rated capacity. The selected numbers and operating conditions of testing batteries are listed in Table 2.

4. Results and discussion

4.1. Computation of SampEn and fitting

The change of surface temperature in charging process generally exhibits a variation tendency with increasing cycling times. Fig. 3 depicts the changes of each cell.

The approach of feature extraction is employed for getting aging information detected from external characteristic curves. Observing the definition and calculation of SampEn, it is obvious that if the maximum distance in Eq. (3) is greater than r, the number will not be changed. SampEn can be keen to variations of some special points which may not be distinctly detected from charging temperature curves. It is worth mentioning that this technique is not sensitive to loss of data and the value does not change due to one or two missing temperature measured points. Otherwise, if the noise signal with large amplitude is added to the measured points, it will be ignored by detection. Parameters directly contribute to the accuracy of functional relationship between SampEn and discharge capacity.

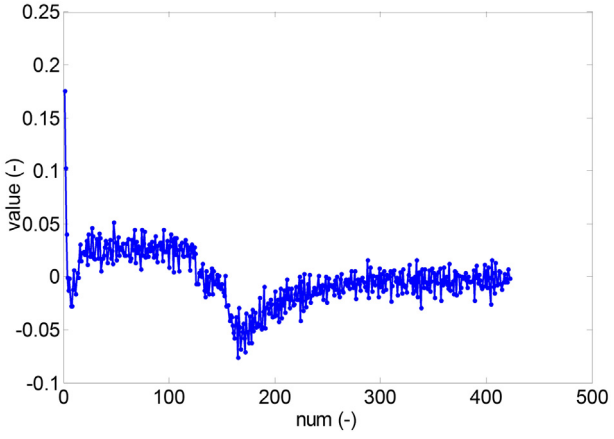

Fig. 4. Curve shape of temperature difference.

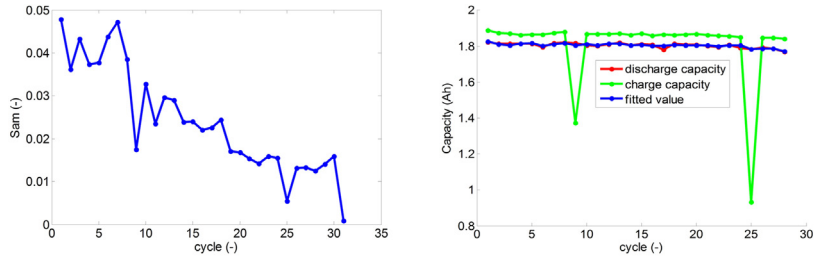

(a) Battery No. 27

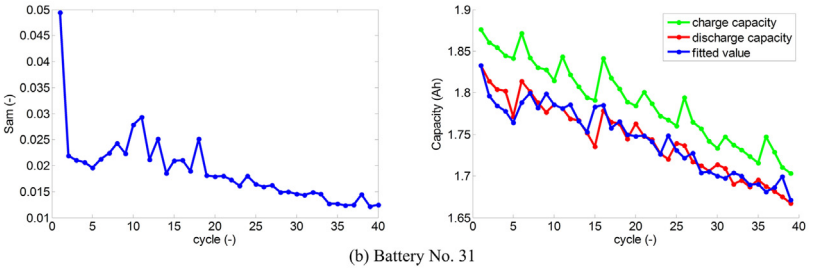

(b) Battery No. 31

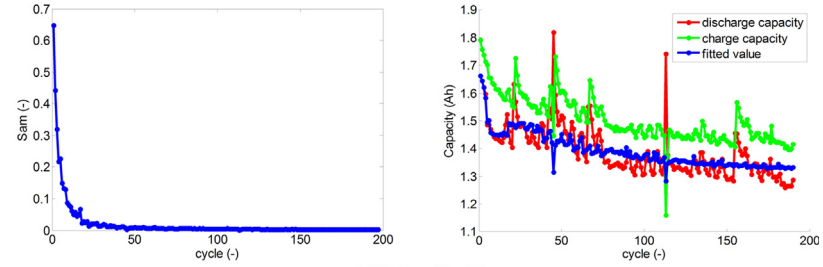

(c) Battery No. 34

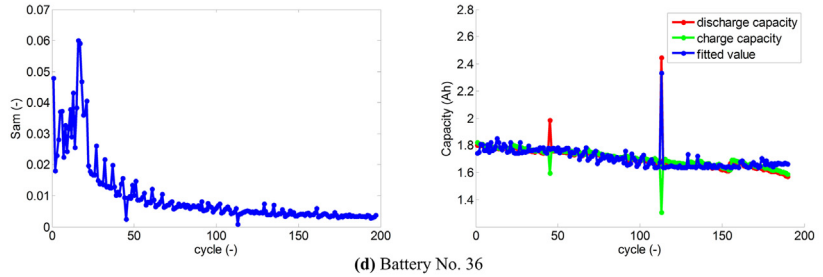

(d) Battery No. 36

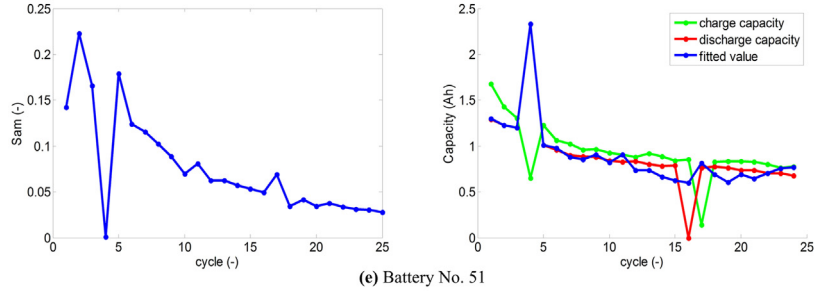

(e) Battery No. 51

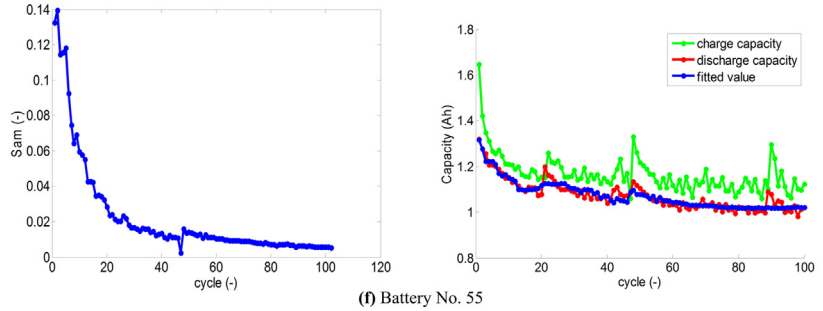

(f) Battery No. 55

Fig. 5. SampEn and fitting results.

Data reacquisition is adopted in this work to decrease the time-consuming of SampEn calculation. Every ten measured points of charging temperature curves are sampled once and generally, the size of N is about 400. Parameter m (typically 2 or 3) is deployed to 4 in our work. According to the computation of SampEn, r is directly related to the temperature difference of adjacent measured points. Fig. 4 roughly depicts the curve shape of temperature difference after data reacquisition. Synthetically considering that improper selected r results in unexpected outcomes, it is deployed to 0.05.

Compared to cubic or six times fitting, nine times fitting results of charging temperature SampEn and discharge capacity show a more accurate and better outcome. Nevertheless, it is inevitable that fitting results can be strongly affected by a sharp increase or decrease in capacity in one cycle. Otherwise, due to the property discrepancy of batteries, fitting parameters display inconsistency and irregularity. Computation of SampEn and nine times fitting results of each cell are shown in Fig. 5.

Fitting results show that variations of temperature difference can depict the capacity fading tendency, which leaves room for further refining in precision. Since charge capacity does not entirely determine nor reflect practical discharge capability, a more sophisticated approach of fitting is presented. All of the three factors including charge capacity, rest time, and temperature SampEn are taken into account.

4.2. Results of estimation

The specific functional expression is obtained by fitting and the results are given in Fig. 6.

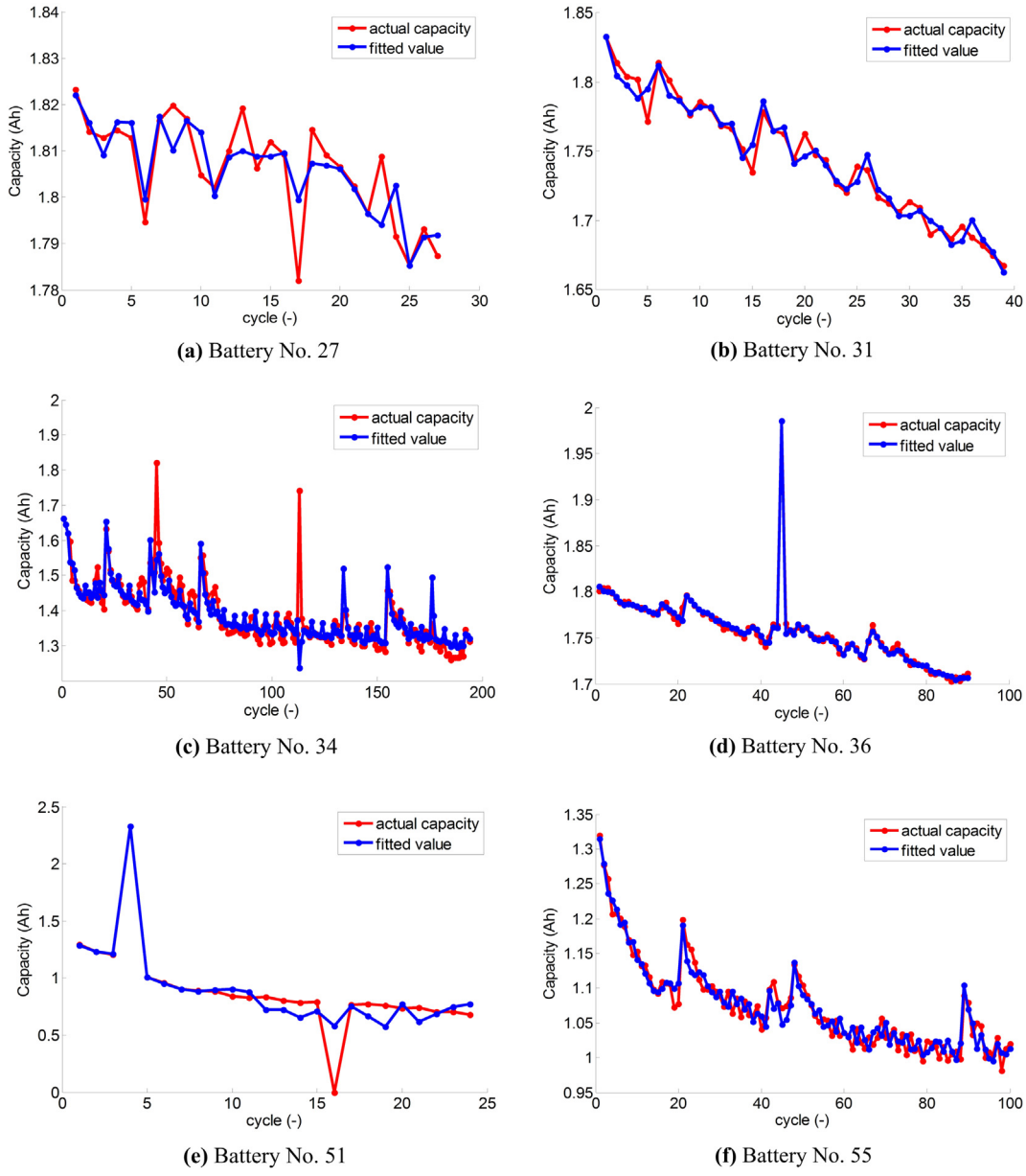

Fig. 6. Fitting results using multi-variable.

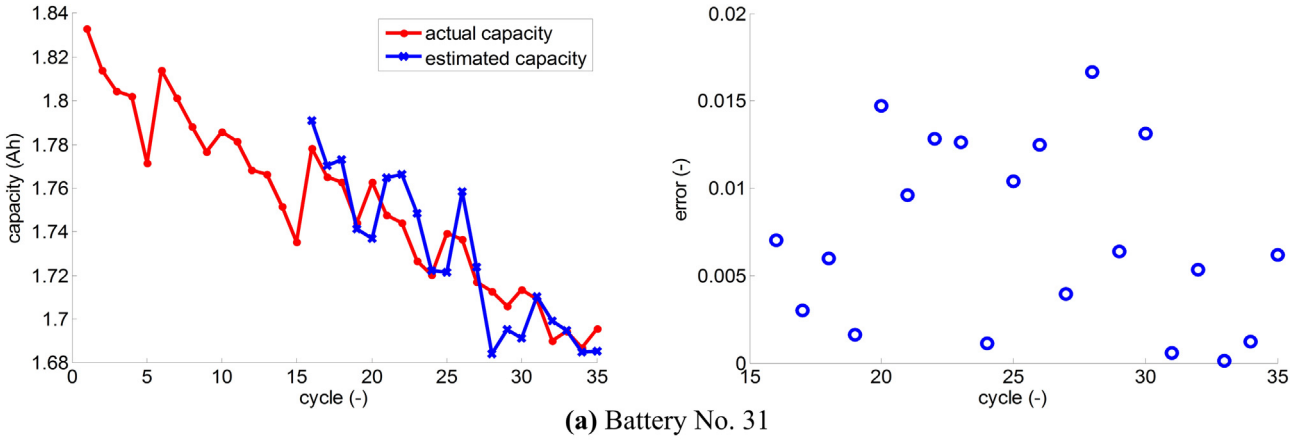

(a) Battery No. 31

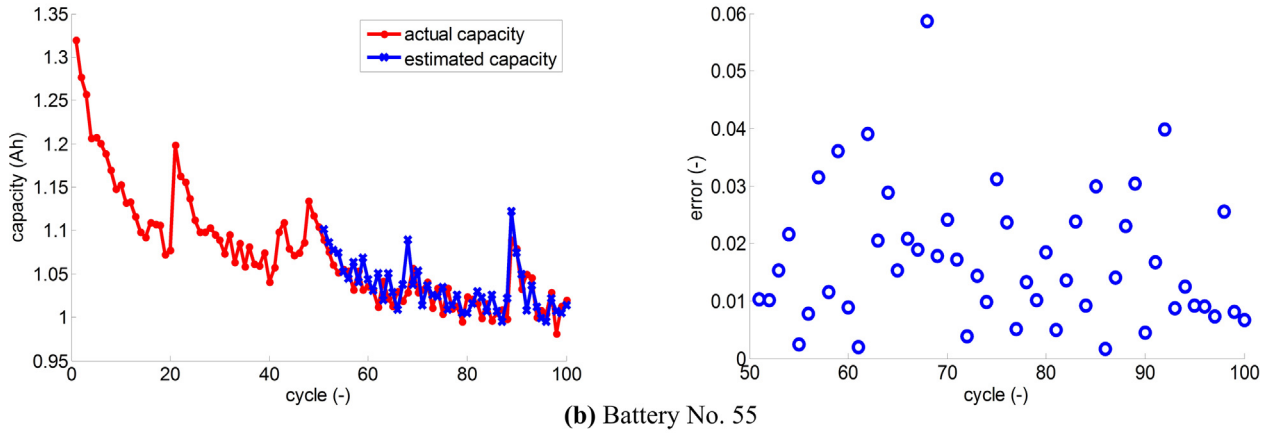

(b) Battery No. 55

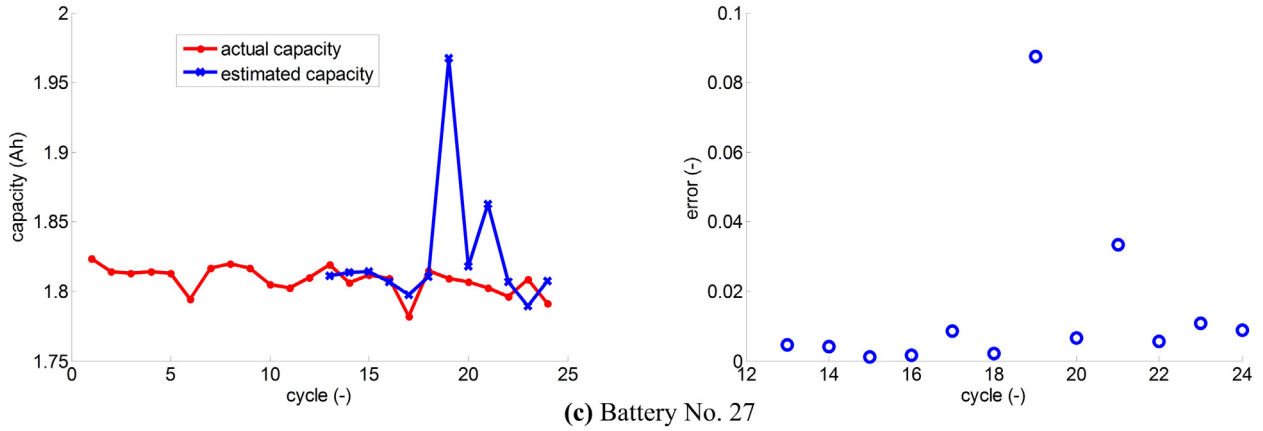

(c) Battery No. 27

Fig. 7. Estimation results and errors of each battery.

$$\begin{aligned}\text{dis\_cha} = {} & a1(\text{Sam\_en})^8 + a2(\text{Sam\_en})^7 + a3(\text{Sam\_en})^6 \\ & + a4(\text{Sam\_en})^5 + a5(\text{Sam\_en})^4 + a6(\text{Sam\_en})^3 \\ & + a7(\text{Sam\_en})^2 + a8(\text{Sam\_en}) + a9 + a10\text{Cha\_cap} \\ & + a11e^{(a12/\text{settime})}\end{aligned} \tag{9}$$

where, $a1-a12$ are parameters, Sam_en, Cha_cap, settime, and dis_cha represent SampEn, charge capacity, rest time, and discharge capacity, separately.

It is evident that multi-variable fitting has a better effect. Based on ideas of feature extraction and modeling, an approach of remaining capacity estimation is proposed. Dynamic fitting result can serve as an indicator for assessing the condition of battery in PF algorithm mentioned in Section 2.3.2.

In this work, three typical operation conditions (B31, B55, and B27) are selected and the data set is divided into two parts. One is used for training or fitting and the other is for validation. Fig. 7 shows the estimation results.

Average relative errors of estimation capacity of each battery are 0.74%, 1.7%, and 1.38%. Apart from individual long time intervals between charging and discharging processes, most intervals are less than 1 h. Insufficient data account for major errors in some estimated points (such as 28th cycle of B31, 68th cycle of B55, and 19th and 21st cycle of B31). Such errors can be

avoided and eliminated with gradual accumulation of historical data.

5. Conclusions

In this work, aging information is extracted from charging temperature curves. A functional relationship between multi-variable factors and discharge capacity is established. The advantages of SampEn and PF are taken to propose a method of remaining capacity estimation. In terms of estimation results on three typical operating conditions, the proposed approach has little average relative errors and exhibits a fine application potential.

Additionally, though the results are satisfactory, there is still considerable space for further improvements. Fused with battery failure mechanisms, the discovery of correlation between aging features and capacity fading will enhance the accuracy of estimation.

Acknowledgment

This research is financially supported by the National Natural Science Foundation of China (no. 51107021) and the Fundamental Research Funds for the Central Universities (grant no. HIT. NSRIF. 2014021). We sincerely appreciate the significant help on translation supported by Miss. Han Wang.

References

[1] W. Kai, Z. Yao, Z. Yuqun, S. Shigang, Prog. Chem. 23 (2–3) (2011) 401–409. http://en.cnki.com.cn/Article_en/CJFDTOTAL-HXJZ2011Z1017.htm.

[2] P. Biensan, B. Simon, J.P. Peres, A. De Guibert, M. Broussely, J.M. Bodet, F. Perton, J. Power Sources 81 (1999) 906–912. http://dx.doi.org/10.1016/S0378-7753(99)00135-4.

[3] J. Vetter, P. Novak, M.R. Wagner, C. Veit, K.C. Möller, J.O. Besenhard, A. Hammouche, J. Power Sources 147 (1) (2005) 269–281. http://dx.doi.org/10.1016/j.jpowsour.2005.01.006.

[4] P. Arora, M. Doyle, R.E. White, J. Electrochem. Soc. 146 (10) (1999) 3543–3553, http://dx.doi.org/10.1149/1.1392512.

[5] M. Dubarry, B.Y. Liaw, M.S. Chen, S.S. Chyan, K.C. Han, W.T. Sie, S.H. Wu, J. Power Sources 196 (7) (2011) 3420–3425. http://dx.doi.org/10.1016/j.jpowsour.2010.07.029.

[6] M. Dubarry, C. Truchot, B.Y. Liaw, K. Gering, S. Sazhin, D. Jamison, C. Michelbacher, J. Power Sources 196 (23) (2011) 10,336–10,343. http://dx.doi.org/10.1016/j.jpowsour.2011.08.078.

[7] M. Pecht, Prognostics and Health Management of Electronics, John Wiley & Sons, Ltd., 2008. 10.1002/9780470061626.shm118.

[8] M. Abbas, A.A. Ferri, M.E. Orchard, G.J. Vachtsevanos, An intelligent diagnostic/prognostic framework for automotive, Intell Veh Symp (2007, June) 352–357, http://dx.doi.org/10.1109/IVS.2007.4290139, 2007 IEEE.

[9] B. Saha, K. Goebel, Modeling Li-ion battery capacity depletion in a particle filtering framework. In: Proceedings of the Annual Conference of the Prognostics and Health Management Society (2009 September).

[10] K. Goebel, B. Saha, A. Saxena, J.R. Celaya, J.P. Christophersen, IEEE Instrum. Meas. Magazine 11 (4) (2008) 33. ftp://labattmot.ele.ita.br/ele/jpenna/Docs_Gerais/Textos/Textos%20Lidos/NASA/1460%20(Goebel).pdf.

[11] B. Saha, S. Saha, K. Goebel, A distributed prognostic health management. In: Proceedings of MFPT, 2009 (2009). Available from: http://www.researchgate.net/publication/228358765_A_Distributed_Prognostic_Health_Management_Architecture/file/9fcfd50d0aafeb75db.pdf.

[12] B. Saha, K. Goebel, J. Christophersen, Trans. Inst. Meas. Control 31 (3, 4) (2009) 293–308. http://tim.sagepub.com/content/31/3-4/293.short.

[13] A.J. Salkind, C. Fennie, P. Singh, T. Atwater, D.E. Reisner, J. Power Sources 80 (1) (1999) 293–300. http://dx.doi.org/10.1016/S0378-7753(99)00079-8.

[14] J. Gomez, R. Nelson, E.E. Kalu, M.H. Weatherspoon, J.P. Zheng, J. Power Sources 196 (10) (2011) 4826–4831. http://dx.doi.org/10.1016/j.jpowsour.2010.12.107.

[15] B.Y. Liaw, R.G. Jungst, G. Nagasubramanian, H.L. Case, D.H. Doughty, J. Power Sources 140 (1) (2005) 157–161. http://dx.doi.org/10.1016/j.jpowsour.2004.08.017.

[16] Y.H. Sun, H.L. Jou, J.C. Wu, Intelligent, Intell. Syst. Des. Appl. 2008 (1) (2008 November) 251–256, http://dx.doi.org/10.1109/ISDA.2008.17.

[17] A. Widodo, M.C. Shim, W. Caesarendra, B.S. Yang, Expert Syst. Appl. 38 (9) (2011) 11,763–11,769. http://dx.doi.org/10.1016/j.eswa.2011.03.063.

[18] J. Li, L. Wang, C. Lyu, W. Luo, K. Ma, L. Zhang, Adv. Mech. Eng. 2013 (2013). http://dx.doi.org/10.1155/2013/154831.

[19] J.S. Richman, J.R. Moorman, Am. J. Physiol. Heart Circulatory Physiol. 278 (6) (2000) H2039–H2049. http://ajpheart.physiology.org/content/278/6/H2039.short.

[20] N.J. Gordon, D.J. Salmond, A.F. Smith, Novel approach to nonlinear, IEE Proc. F. 140 (2) (1993 April) 107–113, http://dx.doi.org/10.1049/ip-f-2.1993.0015.